PCCP

Accepted Manuscript

ROYAL SOCIETY OF CHEMISTRY

www.rsc.org/pccp

Graphene Networks and Its Role on Free-Volume Properties of Graphene/Epoxidied Natural Rubber Composites with a Segregated Structure: Rheological and Positron Annihilation Studies

Canzhong He [a,b,c], Xiaodong She [b,c,*], Zheng Peng [a,c*], Jieping Zhong[a], Shuangquan Liao[b], Wei Gong [a], Jianhe Liao[b] and Lingxue Kong [c]

[a] Chinese Agricultural Ministry Key Laboratory of Tropical Crop Product Processing, Agricultural Product Processing Research Institute, Chinese Academy of Tropical Agricultural Sciences, Zhanjiang 524001, PR China

[b] College of Materials and Chemical Engineering, Hainan University, Haikou, 571737, PR China

[c] Institute for Frontier Materials, Deakin University, Waurn Ponds, Geelong VIC 3216, Australia

[*] Corresponding authors. Tel: +61 416 462 459. E-mail: xiaodongshe@icloud.com (Xiaodong She), zpengcatas@126.com (Zheng Peng)

Abstract

Epoxidized natural rubber/graphene (ENR/GE) composites with segregated GE networks were successfully fabricated using latex mixing combined in situ reduced technology. The rheological behavior and electrical conductivity of ENR/GE composites were investigated. At low frequencies, storage modulus (G′) became frequency-independent suggesting a solid-like rheological behavior and the formation of GE networks. According to the percolation theory, the rheological threshold of ENR/GE composites was calculated to be 0.17 vol.%, which was lower than the electrical threshold of 0.23 vol.%. Both percolation thresholds depended on the evolution of the GE networks in the composites. At low GE concentrations (< 0.17 vol.%), GE existed as individual units, while a ‘‘polymer-bridged GE network’’ was constructed in the composites when GE concentrations exceeded 0.17 vol.%. Finally, a “three–dimensional GE network” with percolation conductive paths was formed with a GE concentration of 0.23 vol.%, where remarkable increase in conductivity of ENR/GE composites was observed. The effect of GE on the atom scale free-volume properties of composites were further studied by positron annihilation lifetime spectroscopy and positron age momentum correlation measurements. The motion of ENR chains were retarded by the geometric confinement of “GE networks’’, producing a high-density interfacial region in the vicinity of GE nanoplatelets, which led to a lower ortho-positronium lifetime intensity and smaller free-volume hole size.

1. Introduction

Graphene (GE), a two-dimensional single-atom thick honey-comb lattice with electrical conductivity up to 6000 S/cm，has attracted enormous scientific interest since its discovery by Novoselov et al [1]. Recently, studies have been conducted on elastomer/GE composites owing to their potential applications in stretchable conductors, electromagnetic shielding devices and many other fields [2-4]. Generally, insulating rubber matrices can be changed into electrical conductor by loading conductive fillers such as GE [5-9], carbon nanotube [10-16], carbon fiber [17-18] and carbon black [19-21]. However, compared to other conductive fillers, GE is superior as a lower loading of GE can lead to a great conductivity of elastomer/GE composites, especially when the GE nanoplatelets are finely dispersed in the matrix with strong interfacial interactions.

The electrical percolation threshold of GE composites strongly depends on the state of GE dispersion, the interactions between GE and polymer chains [22-25]. For example, a lower threshold of 0.17 vol.% was reported by Yu et al. [26-27] for polystyrene/GE composites, where styrene maleic anhydride copolymer was utilized as a compatibilizer. The very low threshold was attributed to the well-dispersed GE sheets and strong interfacial interactions between GE sheets and the polystyrene. More interestingly, Xia et al. [28-29] have found that a “segregated” GE network structure can lead to a low conductivity threshold (0.62 vol.%) of natural rubber/GE composites that synthesized via a latex mixing technology. Similar observations were also

reported by Ruoffs et al. [30-31]. Therefore, in addition to the dispersion status and the interfacial interaction, the structure of GE networks is also very important for revealing the conductive properties of GE composites.

Dynamic rheological properties can provide insights into the evolution of the structure of GE networks, interactions between GE and polymer chains, and the dispersion of GE sheets. Based on this, some interesting rheological properties of elastomer/GE composites were reported, for example, the transition from liquid-like to solid-like rheological behavior, transition from Newtonian to non-Newtonian behavior and strong shear thinning behavior [26-27, 32-34]. In spite of the attention received by this field, the electric conductivity and viscoelastic properties of elastomer/GE composites have been often studied separately. It is of profound importance to systematically reveal the relationship between conductivity and viscoelastic properties.

On the other hand, a precise analysis and characterization of the polymer-filler interface structure at microscopic scale or molecular level is strongly required for the rational design of high performance composite materials. The presence of interfacial interactions between GE and polymer matrix have been well-studied by neutron scattering, nuclear magnetic resonance (NMR), and differential scanning calorimetry (DSC) techniques. Transmission electron microscopy (TEM) and X-ray diffraction (XRD) have been widely used to characterize the dispersion of GE nanoplatelets [2,

35-36]. Notwithstanding numerous experimental and theoretical investigations focus on the characterization of the polymer-filler interface structure, few reports study the effect of dispersed GE nanoplatelets on the chain motions and atom scale free-volume properties of GE based polymer composites, due to the short time scale for dynamic chain motions and the lack of suitable probes for subnanometer molecular dimensions. Recently, positron annihilation lifetime spectroscopy (PALS) as one of the most powerful molecular-scale probes has been employed to characterize the free-volume properties of composites due to its high sensitivity at the subnanometer and subnanosecond ranges [10, 37-40].

In this paper, the evolution of GE networks in epoxidized natural rubber (ENR) and its influence on the mobility of macromolecular chains were systematic investigated. The relationship between rheological percolation, electrical percolation and the structure of GE networks were well elucidated. Furthermore, the atom-scale microstructure of ENR/GE composites was investigated by PALS and Positron age momentum correlation (AMOC) measurements.

2. Experimental

2.1 Materials

Natural rubber latex (NRL) was supplied by Qianjin State Rubber Farm (Zhanjiang, PR China). Flake graphite (average particle size<20 μm, purity>99.9%) was purchased from Qingdao Graphite Co. Ltd (Qingdao, PR China). The reagents

including concentrated sulfuric acid, potassium permanganate, formic acid, hydrazine hydrate, hydrogen peroxide, sodium nitrate and ethyl alcohol were all analytical grade and purchased from Shanghai Chemical Co. Ltd. (Shanghai, PR China).

2.2 Preparation of ENR/GE composites

Graphene oxide (GO) and epoxidized natrual rubber latex (ENRL) were prepared according to our previous published works [5, 41], and the experimental details were fully illustrated in the Supporting Information (SI). A certain amount of GO dispersion was added into the ENR latex under mechanical stirring and ultrasonic irradiation for 4 h to obtain ENR/GO latex (mechanical stirring and ultrasonic irradiation were applied alternately every 30 min). The light brown ENR/GO latex was then in situ reduced by hydrazine hydrate (the weight ratio of hydrazine hydrate to GO was 1:1) under mechanical stirring and ultrasonic irradiation alternately every 30 min for 4 h to obtain black ENR/GE latex. The ENR/GE latex was co-coagulated with ethyl alcohol and the precipitate was soaked in deionized water for 24 hours. Finally the precipitate was dried in a vacuum oven under nitrogen (N_2) atmosphere at 70 °C until equilibrated weight was obtained. During this step, the hydrazine hydrate was removed. The static hot-press samples (with a thickness of 1 mm) were prepared by a vacuum hot-press mold at 155 °C under a pressure of 12 MPa for 15 min and quenched by ice water. The ENR/GE composites with different GE concentration were abbreviated as ENR/GE-0.07, ENR/GE-0.14, ENR/GE-0.28, ENR/GE-0.56, ENR/GE-1.12, ENR/GE-2.24 and ENR/GE-3.36 corresponding to a GE content of

0.07 vol.%, 0.14 vol.%, 0.28 vol.%, 0.56 vol.%, 1.12 vol.%, 2.24 vol.% and 3.36 vol.%, respectively.

2.3 Characterization

TEM digital micrographs were obtained with a JEOL 2010F (JEOL Ltd., Japan) at 200 kV. For solid samples, thin sections (about 70 nm) were cut with an EM-UC6+FC6 cryoultramicrotome (Leica Microsystems, Germany) using a diamond knife (Biel, Switzerland). The chamber temperature is -120 °C and the knife temperature is -95 °C. Sections were collected onto 300 mesh gilder grids from Ted Pella. For latex samples, the composite latex was diluted 22 times and coated onto a copper grid.

Rheological measurements were conducted with a strain-controlled rheometer (ARES-G2, TA instruments, USA) at 180 °C under N_2 protection. The frequency (ω) sweep was measured from 0.01 to 100 rad/s at stress amplitude within linear viscoelastic region of 0.3%. The dynamic time sweep was performed with a frequency of 10 rad/s.

Electrical conductivities were measured with a programmable electrometer (Keithley 617, Keithley Instrucments Inc., USA) via volume resistivity method. Two copper electrodes (Filssynflex Thernko 300H, d=0.3 mm) were attached to sample surfaces. The electric conductivity σ were calculated from the following equation,

$$\sigma = {}^{1}/_{\rho} = d/RS$$

where ρ is the electrical resistivity, d is the thickness of the samples, R is the electrical resistance, and S is the cross section area of the sample.

Positron annihilation lifetime spectroscopy (PALS) measurements were tested by a conventional fast–fast coincidence spectrometer which consists of plastic scintillation detectors with a time resolution of about 290 ps at room temperature. The positron source ^{22}Na (20 μCi) was deposited on a 6μm thick kapton foils and then sandwiched between pieces of identical samples (with a diameter of 1 cm and a thickness of 0.15 cm). Analysis of positron lifetime spectra were performed using finite-term lifetime analysis PATFIT program [42] and continuous-lifetime analysis CONTIN program [43]. Positron age momentum correlation (AMOC) measurements were conducted by acquiring the Doppler broadening and positron lifetime data coincidently [44]. The positron source ^{22}Na (40 μCi) was deposited on a 6 μm thick kapton foils and then sandwiched between samples. The birth signal and the annihilation signal were acquired using a coincidence set-up having two BaF_2 scintillation detectors placed at 90°. A high-purity HPGe detector was placed opposite to the BaF_2 detector. A time resolution of 250 ps FWHM was obtained. The data analysis were fully illustrated in the Supporting Information (SI)

3. Results and Discussion

3.1 Dispersion of GE nanoplatelets within composites

In our provious work [41], a molecular-level dispersion of GO within epoxidied natural rubber matrix was achieved by enhancing the interfacial interaction between GO and the rubber matrix. In particular, restacking and agglomeration of GO sheets were successful depressed via hydrogen bonding between the epoxy, hydroxyl groups of ENR and oxygenous groups of GO. Therefore, in order to preserve the homogeneous dispersion of the fillers within the rubber matrix, the ENR/GO composites were in situ reduced by hydrazine hydrate to obtain highly stretchable and electrical conductive ENR/GE composites.

The morphology and dispersion of the GE nanoplatelets in ENR are revealed by TEM micrography. At low GE concentrations, monolayer GE nanoplatelets were attached onto the surface of ENR particles, and the wrinkled GE nanoplatelets were homogeneously dispersed throughout the ENR matrix as shown in Fig. 1a and a'. The wrinkled structure will help to increase the inter-plate connectivity to form a three-dimensional conductive GE network and is valuable in reducing reaggregations [32, 45]. With an increase in the concentration of GE, a "core-shell" structure, where compactly interconnected GE shell coated on the surface of the ENR particles, was found (Fig. 1b and c). In addition, "segregated GE networks" was observed within the composites (Fig. 1b' and c'). The interstitial areas between ENR particles act as a template for the formation of the "segregated networks". As demonstrated by Xia et al.[28] and Ruoff et al.[30], the "segregated structure" is important for the formation of conducting networks with a lower content of fillers.

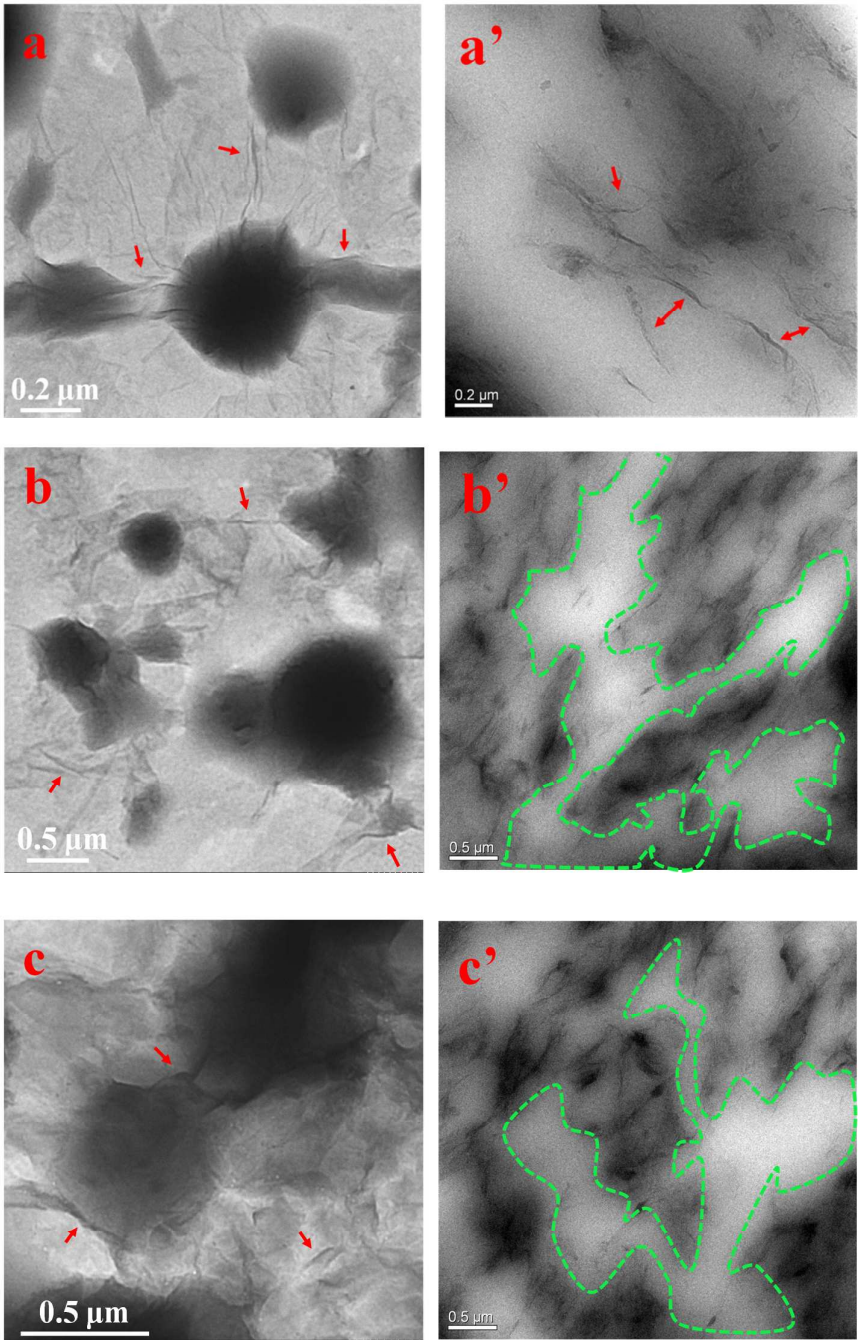

Fig. 1 TEM micrography of ENR/GE latex (a–c) and ENR/GE solid composites (a'–c') with different GE loadings. (a, a') ENR/GE–0.07, (b, b') ENR/GE–0.28 and (c, c') ENR/GE–0.56.

3.2 Rheological networks

It is accepted that complex viscosity (| η^*|) and dynamic storage modulus (G′) are extremely sensitive to the microstructure variation of nanofiller reinforced polymer composites. As shown in Fig. 2a and b, the addition of GE leads to the appreciable enhancements in both | η^*| and G′ of ENR/GE composites in comparison to those of neat ENR. This effect is most pronounced at low frequencies and diminishes with an increase in the frequency. It is worthy notice that the viscosity curves of ENR/GE composites with a GE loading of 0.07 and 0.14 vol.% significantly show Newtonian plateau at low frequencies, while this plateau moves to lower frequencies when the GE loading exceeds 0.14 vol.%. This observation is due to the strong shear thinning behavior, which is accordance with observations found within the layered silicates/polymer systems [46-51] and carbon nanotube/polymer systems [10-12, 52-54].

The increase of the | η^*| of ENR/GE composites is due to the increase of G′ and loss modulus (G″) [10, 53]. The low frequency slopes of G′ and G″ are listed in Table 1. It is found that for neat ENR, $G' \propto \omega^{1.87}$ and $G'' \propto \omega^{0.92}$, which greatly follow the linear rheological theory ($G' \propto \omega^2$ and $G'' \propto \omega^1$). This result demonstrates that the ENR molecular chains are fully relaxed and exhibit a terminal behavior. Nevertheless, the low frequency slopes of G′ and G″ decrease monotonically with increasing GE content. When the GE loadings exceeds 0.14 vol.%, there is a sharp falling from 1.56 to 0.56 for G′ and from 0.89 to 0.53 for G″, indicating that the ENR/GE composites

exhibit a non-terminal solid-like viscoelastic behavior. This phenomenon can be attributed to the formation of GE networks which restricts the long-range motion of the ENR chains. At high frequencies, the effect of the GE loading on the rheological behavior is relatively weak，suggesting that GE nanoplatelets do not exert an significant influence on the short-range dynamics of the ENR chains [12, 52].

Table 1 Rheological fitting results of ENR/GE composites

	Low-freq slope of G′ vs ω	Low-freq slope of G″ vs ω	Time-dependent exponent β
ENR	1.87	0.92	-
ENR/GE-0.07	1.64	0.89	0.046
ENR/GE-0.14	1.56	0.89	0.054
ENR/GE-0.28	0.56	0.53	0.167
ENR/GE-0.56	0.51	0.47	0.221
ENR/GE-1.12	0.38	0.45	0.223
ENR/GE-2.24	0.27	0.38	0.334
ENR/GE-3.36	0.19	0.32	0.351

It was proposed that curves of log G′ versus log G″ can be used to indicate microstructure changes between the matrix and filler at a given temperature[10, 55]. As shown in Fig. 2d, when the GE content exceeds 0.14 vol.%, the slopes of the curves change drastically, indicating the significant variation of the microstructure of

composites. Furthermore, Fig. 2e shows the dynamic time sweeps of ENR and ENR/GE composites at a fixed frequency of 10 rad/s. It is appeared that the neat ENR exhibits a good thermal stability during the rheological measurement. At longer time scale (t>7500 s), the storage modulus almost linearly increase with time, implying a power-law scaling, $G' \propto t^{\beta}$ [56-60] and the power-law exponent β evaluated at t=7500~11,000 is listed in Table 1. It is notable from Fig. 1e and Table 1 that the storage modulus G′ and β change significantly when the GE content exceeds 0.14 vol.%，proving the formation and improvement of the GE networks.

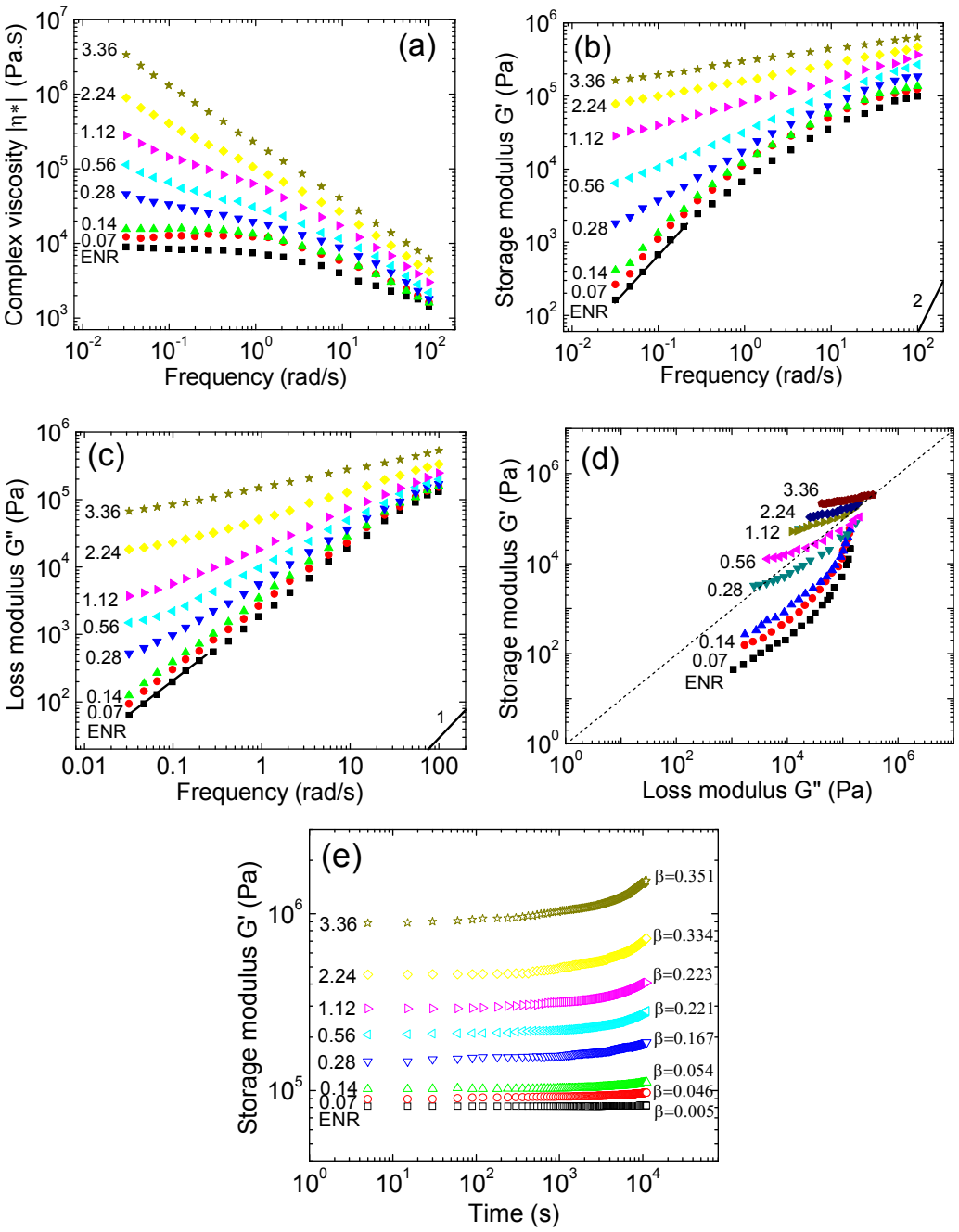

Fig. 2 (a) Complex viscosity | η^*|, (b) storage modulus G′ and (c) loss modulus G″ of the ENR/GE composites as a function of frequency at 180 °C, (d) G′ as a function of G″ of the ENR/GE composites, (e) dynamic time sweeps of ENR/GE composites at a fixed frequency of 10 rad/s.

Based on the above analysis, there should be a critical GE concentration that is attributed to the sudden change in the material microstructure when the GE loading exceed 0.14 vol.%. According to the percolation theory, a power-law relation can be used to determine the rheological percolation threshold [12, 45, 57, 61-62]:

$$G' \propto (\varphi - \varphi_{cG'})^{\tau_{G'}} \qquad (1)$$

where G′ is the low frequency storage modulus, φ is the GE volume fraction, $\varphi_{cG'}$ is the threshold fraction and $\tau_{G'}$ is the critical exponent. According to the double-logarithmic plot, the rheological percolation threshold and critical exponent can be calculated to be 0.17 vol. % and 1.857 (Fig. 3a inset), respectively. Ren[63] and Kim[12, 56]demonstrated that the relationship between the percolation threshold and the aspect ratio (A_f) can be constructed as follow:

$$A_f = \frac{D}{h} = \frac{3\varphi_{sphere}}{2\varphi_p} \qquad (2)$$

where φ_{sphere}=0.29 is the percolation threshold of random packed three-dimensional interpenetrating spheres [64] and φ_p=0.0017 is the onsets of rheological threshold. The average aspect ratio of GE nanoplatelets is calculated to be 255. Due to such a high aspect ratio and length range of 0.5~4 μm (obtained from AFM measurements in Supporting Information, Fig. S1) which is much larger than the entanglement distance of ENR molecular chains and average diameters of the random coils, GE nanoplatelets can act as "obstacles" to block the long-range segmental motions that was also evidenced by the low-frequency non-terminal rheological behavior.

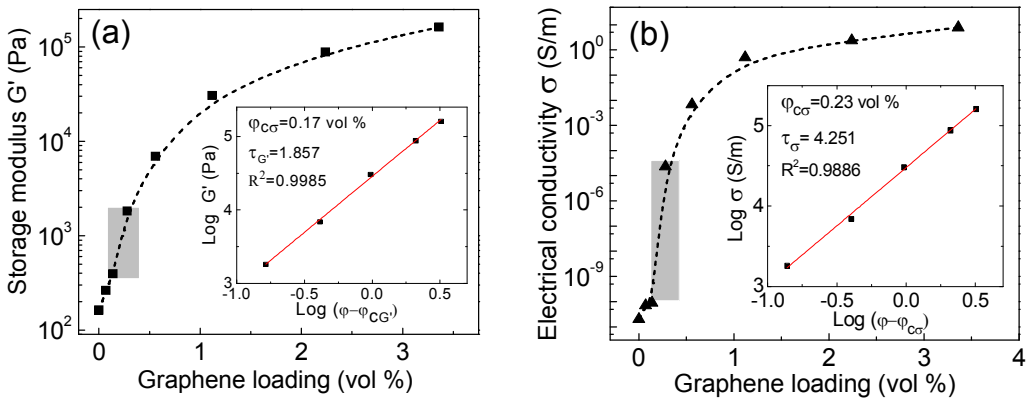

Fig. 3 (a) Storage modulus G′ of the ENR/GE composites as a function of GE loading, the inset is a log-log plot of G′ versus reduced mass fraction, (b) electrical conductivity $\varphi_{c\sigma}$ of the ENR/GE composites as a function of GE loading, the inset is a log-log plot of electrical conductivity versus reduced mass fraction.

3.3 Electrical Conductive networks

The electrical conductivity of the composites strongly depends on the GE loading (Fig. 3b). Particularly, a significant increase between ENR/GE-0.14 and ENR/GE-0.28 is observed. The electrical conductivity percolation threshold ($\varphi_{c\sigma}$) can be determine by a power law relation [65-66].

$$\sigma \propto (\varphi - \varphi_{c\sigma})^{\tau_\sigma} \qquad (3)$$

Where σ represents the electrical conductivity, φ is the GE volume fraction and τ_σ is the critical exponent. The best fitting to the log-log plot of conductivity curve is $\varphi_{c\sigma}$= 0.23 vol. % and τ=4.25 (Fig. 3b inset).

It has been demonstrated that the critical exponent τ only depends on the dimensionality of composites [67]. Particularly, $\tau < 2.1$ indicates the matrix with a

polymer-bridged particle network, whereas $\tau > 3.75$ corresponds to the establishment of a direct particle–particle interaction network within the matrix [32, 61, 68-70]. Therefore, a $\tau_{G'}$ value of 1.86 for ENR/GE composites indicates the formation of a polymer-bridged GE network, which is sensitively detected by dynamical rheological test. On the other hand, a τ_{σ} value of 4.25 indicates the existence of a compactly interconnected GE networks.

It is found that the rheological percolation thresholds (0.17 vol.%) is lower than the electrical thresholds (0.23 vol.%) since the percolation mechanisms are different. In general, rheological percolation requires a larger inter-particle distance (tens of nanometers) while electrical percolation need ~5 nm to achieve electron hopping. In GE/polymer composites, there could be three kinds of networks: (i) temporary entangled polymer network, (ii) combined GE-polymer-GE network and (iii) interconnected GE network. These are schematically illustrated in Fig. 4.

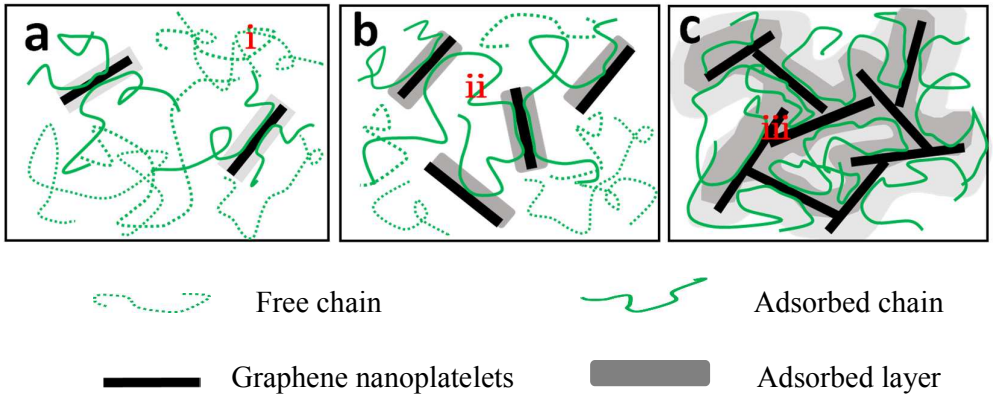

Fig. 4 A simplified scheme for the GE networks evolution and its role on the alteration of chain dynamics in ENR/GE composites.

At low GE concentrations (＜0.17 vol.%), GE sheets exist as individual units rather than connected networks, due to the average distance between them is larger than their own size range (Fig. 4a). This is the reason why the conductivity of the nanocomposites is very close to that of the pure ENR and no significant increase is found in G' of the composites. When the GE concentration reaches the rheological percolation threshold (GE concentration≥ 0.17 vol.%), a ''polymer-bridged GE network'' is constructed in the composites, where polymer chains attach on the surface of GE nanoplatelets and act as "bridges" to connect the GE sheets, causing the depression of the motion of the polymer chains (Fig. 4b). As a result, the rheological properties begin to exhibit a pseudo-solid-like behavior. On the other hand, because only few electrons can be dictated by the thin "polymer bridge layers" surrounding the GE sheets, the electrical conductivity of composites is still very low. When the GE concentration is high enough (≥ 0.23 vol.%) to form a percolation conductive path along the network via directly contact between GE sheets, a "three-dimensional GE network'' structure is constructed and the onset of electrical conductivity percolation threshold is observed. Within this network, the free rotation of GE nanoplatelets is hindered by adjacent ones. Meanwhile, the motion of ENR chains are retarded by the geometric confinement of "three-dimensional GE networks'', forming a high-density interfacial region in the vicinity of GE nanoplatelets as shown in Fig. 4c.

It is found from some representative results shown in Table S1, the electrical behavior

of ENR/GE composites presented here is better than those reported in the literatures. Such a low electrical threshold and high value of critical exponent can be attributed to the wrinkled structure and high aspect ratio of GE nanaplatelets, well designed "three-dimensional segregated GE networks" in ENR matrix, and the strong interfacial interaction between GE and ENR matrix.

3.4 The influence of GE networks on the free-volume properties

Dynamical rheological and electrical conductivity measurements illustrate that GE nanoplatelets exert a considerable effect on the microstructure of ENR/GE composites. PALS is certainly a useful technique to study local segmental motion and packing at the molecular level [37]. The variation of ortho-positronium (*o*-Ps) lifetime (τ_3) and o-Ps intensity (I_3) of ENR/GE composites as a function of GE loading are showed in Fig. 5.

The *o*-Ps lifetime τ_3 monotonously decreases with the increasing GE loading. This decrease in τ_3 mirrors the decrease of the average size of free volume cavities where *o*-Ps localized and annihilated. This may be interpreted by two reasons. Firstly, as mentioned above, the strong interfacial interactions between GO and ENR matrix and the "obstacles effect" caused by GE nanoplatelets can effectively restrain the motion of ENR chains. Secondly, the introduction of monolayer GE nanosheets into ENR matrix results in an occupancy of a significant fraction of pores [10, 71]. It is more intriguing to observe a sharp falling of I_3 between ENR/GE-0.14 and ENR/GE-0.28,

indicating that there is a change in the microstructure of composites [72-73]. This observation is greatly corroborated with the rheological and electrical conductivity measurements. When GE network is constructed, the mobility and relaxation of macromolecular chains are restricted within the mesoscopic GE networks and this produces a high-density interfacial region in the vicinity of GE, leading to the dramatically decrease in the free-volume concentration. At the same time, owning to the construction of the GE network, the rheological properties exhibit a pseudo-solid-like behavior and a better electrical conductivity of the composites was found.

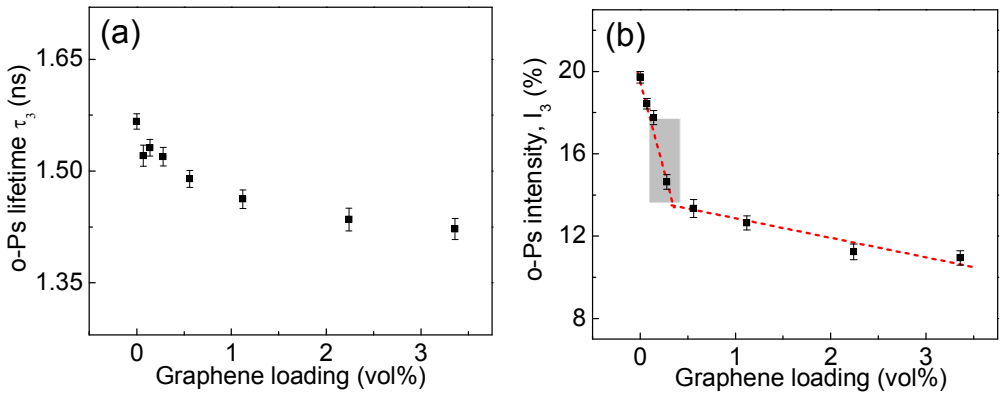

Fig. 5 The effect of GE loading on (a) *o*-Ps lifetime τ_3 and (b) *o*-Ps intensity I_3 of ENR/GE composites.

The *o*-Ps annihilation lifetime distributions obtained from CONTIN analysis can be transformed into free-volume hole distributions according to equation (4) and (5) [74-76].

$$\tau_{o-Ps} = \frac{1}{2}\left[1 - \frac{R}{R+\Delta R} + \frac{1}{2\pi}\sin\left(\frac{2\pi R}{R+\Delta R}\right)\right]^{-1} \quad (4)$$

$$V_f(\mathrm{pdf}) = -3.32\left\{\cos\left[\frac{2\pi R}{R+1.66}\right]-1\right\}\alpha(\lambda)/\{(R+1.66)^2K(R)4\pi R^2\} \qquad (5)$$

Where $\tau_{o\text{-Ps}}$ represents o-Ps lifetime, R is the size of free volume holes and $\Delta R = 1.66\text{Å}$ is the fitted empirical electron-layer thickness [75-77]. The free-volume hole probability density function V_f(pdf) is shown in Fig. 6a. The Gaussian-like distributions becomes border and the peak position shifts to a lower value with increasing GE content. The full width at half maximum (FWHM) is 47.3, 49.4, 53.7, 68.4, 73.6 and 82.13 for ENR, ENR/GE-0.07, ENR/GE-0.14, ENR/GE-0.28, ENR/GE-0.56 and ENR/GE-1.12, respectively. It is accepted that ENR/GE composites are multiphase systems providing new possible annihilation sites for positron/Ps, such as, polymer–nanophase interface layers and nanophase (GE). The appearance of lower size free-volume hole can be attributed to the formation of GE networks which provides a high density interfacial region that is missing in the neat ENR.

Positron age–momentum correlation (AMOC) was carried out to elucidate how the positron/Ps annihilation sites were influenced by GE in ENR/GE composites[44, 75]. As shown in Fig. 6b, the changes of S(t) parameter value with the positron age undergo three stages, the self-annihilation of *para*-positronium (*p*-Ps, 0~0.6ns), the "free" positron annihilation (0.6~2ns) and *o*-Ps pick-off annihilation (above 2ns). It is well accepted that the positron age of *o*-Ps (corresponding to τ_3) can be used to track the variation of free-volume holes [75-76]. Within the positron age of *o*-Ps, the S(t) of ENR/GE composites is lower than that of the pure ENR and decreases with an

increase in the GE loading. This observation demonstrates that the addition of GE affects the microstructure of ENR/GE composites which leads to the variation of free-volume holes. In addition, this effect is enhanced with the increasing GE concentration because the formation of GE networks at higher GE concentrations remarkably changes the microstructure of ENR/GE composites. This is the reason why significant changes were observed in the rheological and electrical conductivity properties.

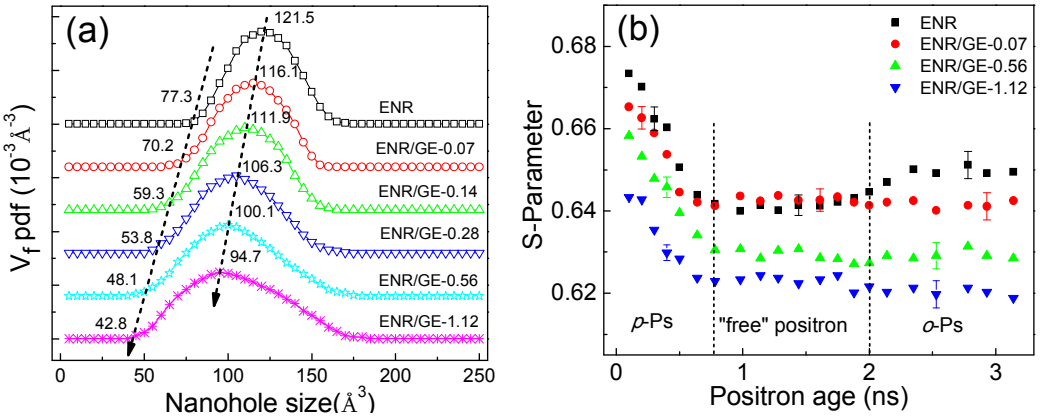

Fig. 6 (a) Free-volume hole distribution for ENR/GE composites evaluated from the CONTIN analysis, (b) Positron-age dependence of the S(t) parameter for ENR/GE composites evaluated from AMOC measurements.

4. Conclusions

Epoxidized natural rubber/graphene (ENR/GE) composites with segregated GE networks were successfully fabricated. The distinct segregated GE networks with wrinkled structure were evidenced by TEM microscopy. The formation of GE networks in the composites had a strong influence on the viscoelastic behavior and

electrical conductivity of ENR/GE composites. According to the threshold theory, the rheological threshold and the electric threshold were determined to be 0.17 vol.% and 0.23 vol.%, respectively. The long-range segmental motion of the ENR chains was suppressed by the addition of GE nanoplatelets, because they have an average aspect ratio of 255 and a length range of 0.5~4 um which was much larger than the average diameter of the entanglement distance of ENR molecular chains. Furthermore, when the GE loading exceeded 0.23 vol.%, a "three-dimensional GE network'' structure with strong interconnected GE sheets was constructed in the composites. Within these networks, the free rotation of GE nanoplatelets was hindered by adjacent ones. Meanwhile, the motion of ENR chains are retarded by the geometric confinement of "GE networks'', producing a high-density interfacial region in the vicinity of GE nanoplatelets. The higher GE nanoplatelets loading, the more restraint on the mobility of ENR chains was observed, which resulted in a larger G' and smaller low-frequency slope of G′ vs ω at low frequency. The PALS and AMOC confirmed that the atom scale free-volume of ENR was dramatically influenced by the formation of GE networks.

Acknowledgments

The financial support from the National Program on Key Basic Research Project of China for 973 Preceding Program (NO.2010CB635109), the National Natural Science Foundation of China (No.50963001), the Fundamental Scientific Research Funds for Chinese Academy of Tropical Agricultural Sciences (CATAS)

(NO.1630062013011) and the Alfred Deakin Postdoctoral Program are gratefully acknowledged. Pengfei Zhao provided help with the TEM experimental works and Dr. Xin Wang provided help with the PALS experimental works, hereby acknowledged.

References

[1] Novoselov KS, Geim AK, Morozov SV, Jiang D, Zhang Y, Dubonos SV, et al. Electric field in atomically thin carbon films. Science. 2004;306(5696):666-9.

[2] Sadasivuni KK, Ponnamma D, Thomas S, Grohens Y. Evolution from graphite to graphene elastomer composites. Progress in Polymer Science. 2014;39(4):749-80.

[3] Young RJ, Kinloch IA, Gong L, Novoselov KS. The mechanics of graphene nanocomposites: A review. Composites Science and Technology. 2012;72(12):1459-76.

[4] Gong L, Kinloch IA, Young RJ, Riaz I, Jalil R, Novoselov KS. Interfacial stress transfer in a graphene monolayer nanocomposite. Advanced Materials. 2010;22(24):2694-7.

[5] Luo Y, Zhao P, Yang Q, He D, Kong L, Peng Z. Fabrication of conductive elastic nanocomposites via framing intact interconnected graphene networks. Composites Science and Technology. 2014;100:143-51.

[6] Matos CF, Galembeck F, Zarbin AJG. Multifunctional and environmentally friendly nanocomposites between natural rubber and graphene or graphene oxide. Carbon. 2014;78:469-79.

[7] Xing W, Tang M, Wu J, Huang G, Li H, Lei Z, et al. Multifunctional properties of

graphene/rubber nanocomposites fabricated by a modified latex compounding method. Composites Science and Technology. 2014;99:67-74.

[8] Tang ZH, Guo BC, Zhang LQ, Jia DM. Graphene/rubber nanocomposites. Acta Polymerica Sinica. 2014(7):865-77.

[9] Tang Z, Wu X, Guo B, Zhang L, Jia D. Preparation of butadiene-styrene-vinyl pyridine rubber-graphene oxide hybrids through co-coagulation process and in situ interface tailoring. Journal of Materials Chemistry. 2012;22(15):7492-501.

[10] Yan X, Gong Z, Gong J, Gao S, Zhang Z, Wang B. Investigation of the rheological and conductive properties of multi-walled carbon nanotube/polycarbonate composites by positron annihilation techniques. Carbon. 2012;50(8):2899-907.

[11] Kim M, Mun SC, Lee CS, Lee MH, Son Y, Park OO. Electrical and rheological properties of polyamide 6,6/γ-ray irradiated multi-walled carbon nanotube composites. Carbon. 2011;49(12):4024-30.

[12] Kim H, Macosko CW. Morphology and properties of polyester/exfoliated graphite nanocomposites. Macromolecules. 2008;41(9):3317-27.

[13] Yu CR, Wu DM, Liu Y, Qiao H, Yu ZZ, Dasari A, et al. Electrical and dielectric properties of polypropylene nanocomposites based on carbon nanotubes and barium titanate nanoparticles. Composites Science and Technology. 2011;71(15):1706-12.

[14] Yan D, Li X, Ma HL, Tang XZ, Zhang Z, Yu ZZ. Effect of compounding sequence on localization of carbon nanotubes and electrical properties of ternary nanocomposites. Composites Part A: Applied Science and Manufacturing. 2013;49:35-41.

[15] Yue D, Liu Y, Shen Z, Zhang L. Study on preparation and properties of carbon nanotubes/rubber composites. Journal of Materials Science. 2006;41(8):2541-4.

[16] Mun SC, Kim M, Prakashan K, Jung HJ, Son Y, Park OO. A new approach to determine rheological percolation of carbon nanotubes in microstructured polymer matrices. Carbon. 2014;67:64-71.

[17] Wu AS, Chou TW. Carbon nanotube fibers for advanced composites. Materials Today. 2012;15(7-8):302-10.

[18] Breuer O, Sundararaj U. Big returns from small fibers: A review of polymer/carbon nanotube composites. Polymer Composites. 2004;25(6):630-45.

[19] Kreyenschulte H, Richter S, Götze T, Fischer D, Steinhauser D, Klüppel M, et al. Interaction of 1-allyl-3-methyl-imidazolium chloride and carbon black and its influence on carbon black filled rubbers. Carbon. 2012;50(10):3649-58.

[20] Luheng W, Tianhuai D, Peng W. Influence of carbon black concentration on piezoresistivity for carbon-black-filled silicone rubber composite. Carbon. 2009;47(14):3151-7.

[21] Krajči J, Špitálský Z, Chodák I. Relationship between conductivity and stress-strain curve of electroconductive composite with SBR or polycaprolactone matrices. European Polymer Journal. 2014;55(1):135-43.

[22] Chen G, Liu Y, Liu F, Zhang X. Fabrication of three-dimensional graphene foam with high electrical conductivity and large adsorption capability. Applied Surface Science. 2014;311:808-15.

[23] Chakraborty I, Bodurtha KJ, Heeder NJ, Godfrin MP, Tripathi A, Hurt RH, et al.

Massive electrical conductivity enhancement of multilayer graphene/polystyrene composites using a nonconductive filler. ACS Applied Materials and Interfaces. 2014;6(19):16472-5.

[24] Li M, Gao C, Hu H, Zhao Z. Electrical conductivity of thermally reduced graphene oxide/polymer composites with a segregated structure. Carbon. 2013;65:371-3.

[25] Qi XY, Yan D, Jiang Z, Cao YK, Yu ZZ, Yavari F, et al. Enhanced electrical conductivity in polystyrene nanocomposites at ultra-low graphene content. ACS Applied Materials and Interfaces. 2011;3(8):3130-3.

[26] Zhang HB, Zheng WG, Yan Q, Jiang ZG, Yu ZZ. The effect of surface chemistry of graphene on rheological and electrical properties of polymethylmethacrylate composites. Carbon. 2012;50(14):5117-25.

[27] He Z, Zhang B, Zhang HB, Zhi X, Hu Q, Gui CX, et al. Improved rheological and electrical properties of graphene/polystyrene nanocomposites modified with styrene maleic anhydride copolymer. Composites Science and Technology. 2014;102:176-82.

[28] Zhan Y, Lavorgna M, Buonocore G, Xia H. Enhancing electrical conductivity of rubber composites by constructing interconnected network of self-assembled graphene with latex mixing. Journal of Materials Chemistry. 2012;22(21):10464-8.

[29] Zhan Y, Wu J, Xia H, Yan N, Fei G, Yuan G. Dispersion and exfoliation of graphene in rubber by an ultrasonically- assisted latex mixing and in situ reduction process. Macromolecular Materials and Engineering. 2011;296(7):590-602.

[30] Potts JR, Shankar O, Du L, Ruoff RS. Processing-morphology-property relationships and composite theory analysis of reduced graphene oxide/natural rubber nanocomposites. Macromolecules. 2012;45(15):6045-55.

[31] Potts JR, Dreyer DR, Bielawski CW, Ruoff RS. Graphene-based polymer nanocomposites. Polymer. 2011;52(1):5-25.

[32] Sabzi M, Jiang L, Liu F, Ghasemi I, Atai M. Graphene nanoplatelets as poly(lactic acid) modifier: Linear rheological behavior and electrical conductivity. Journal of Materials Chemistry A. 2013;1(28):8253-61.

[33] Niu R, Gong J, Xu D, Tang T, Sun ZY. Influence of molecular weight of polymer matrix on the structure and rheological properties of graphene oxide/polydimethylsiloxane composites. Polymer (United Kingdom). 2014;55(21):5445-53.

[34] Basu S, Singhi M, Satapathy BK, Fahim M. Dielectric, electrical, and rheological characterization of graphene-filled polystyrene nanocomposites. Polymer Composites. 2013;34(12):2082-93.

[35] Kuilla T, Bhadra S, Yao D, Kim NH, Bose S, Lee JH. Recent advances in graphene based polymer composites. Progress in Polymer Science (Oxford). 2010;35(11):1350-75.

[36] Li C, Feng C, Peng Z, Gong W, Kong L. Ammonium-assisted green fabrication of graphene/natural rubber latex composite. Polymer Composites. 2013;34(1):88-95.

[37] Jean YC, Van Horn JD, Hung WS, Lee KR. Perspective of positron annihilation spectroscopy in polymers. Macromolecules. 2013;46(18):7133-45.

[38] Yan X, Gong Z, Gong J, Gao S, Wang B, Ruan X. Investigation of the glass transition and viscoelastic properties of polycarbonate/multi-walled carbon nanotube composites by positron annihilation lifetime spectroscopy. Polymer (United Kingdom). 2013;54(2):798-804.

[39] Frielinghaus X, Brodeck M, Holderer O, Frielinghaus H. Confined polymer dynamics on clay platelets. Langmuir. 2010;26(22):17444-8.

[40] Harms S, Rätzke K, Faupel F, Schneider GJ, Willner L, Richter D. Free volume of interphases in model nanocomposites studied by positron annihilation lifetime spectroscopy. Macromolecules. 2010;43(24):10505-11.

[41] She X, He C, Peng Z, Kong L. Molecular-level dispersion of graphene into epoxidized natural rubber: Morphology, interfacial interaction and mechanical reinforcement. Polymer. 2014;55(26):6803-10.

[42] Kirkegaard P, Eldrup M, Mogensen OE, Pedersen NJ. Program system for analysing positron lifetime spectra and angular correlation curves. Computer Physics Communications. 1981;23(3):307-35.

[43] Gregory RB, Zhu Y. Analysis of positron annihilation lifetime data by numerical laplace inversion with the program CONTIN. Nuclear Inst and Methods in Physics Research, A. 1990;290(1):172-82.

[44] Sato K, Murakami H, Ito K, Hirata K, Kobayashi Y. Positron age-momentum correlation studies of free volumes in polymers. Radiation Physics and Chemistry. 2009;78(12):1085-7.

[45] Kim H, Abdala AA, Macosko CW. Graphene/polymer nanocomposites.

Macromolecules. 2010;43(16):6515-30.

[46] Wang K, Liang S, Deng J, Yang H, Zhang Q, Fu Q, et al. The role of clay network on macromolecular chain mobility and relaxation in isotactic polypropylene/organoclay nanocomposites. Polymer. 2006;47(20):7131-44.

[47] Gelfer MY, Burger C, Chu B, Hsiao BS, Drozdov AD, Si M, et al. Relationships between structure and rheology in model nanocomposites of ethylene-vinyl-based copolymers and organoclays. Macromolecules. 2005;38(9):3765-75.

[48] Ren J, Krishnamoorti R. Nonlinear viscoelastic properties of layered-silicate-based intercalated nanocomposites. Macromolecules. 2003;36(12):4443-51.

[49] Ray SS, Okamoto K, Okamoto M. Structure-property relationship in biodegradable poly(butylene succinate)/layered silicate nanocomposites. Macromolecules. 2003;36(7):2355-67.

[50] Zhang Q, Archer LA. Poly(ethylene oxide)/silica nanocomposites: Structure and rheology. Langmuir. 2002;18(26):10435-42.

[51] Solomon MJ, Almusallam AS, Seefeldt KF, Somwangthanaroj A, Varadan P. Rheology of polypropylene/clay hybrid materials. Macromolecules. 2001;34(6):1864-72.

[52] Du F, Scogna RC, Zhou W, Brand S, Fischer JE, Winey KI. Nanotube networks in polymer nanocomposites: Rheology and electrical conductivity. Macromolecules. 2004;37(24):9048-55.

[53] Sung YT, Han MS, Song KH, Jung JW, Lee HS, Kum CK, et al. Rheological and

electrical properties of polycarbonate/multi-walled carbon nanotube composites. Polymer. 2006;47(12):4434-9.

[54] Kim KS, Rhee KY, Lee KH, Byun JH, Park SJ. Rheological behaviors and mechanical properties of graphite nanoplate/carbon nanotube-filled epoxy nanocomposites. Journal of Industrial and Engineering Chemistry. 2010;16(4):572-6.

[55] Pötschke P, Fornes TD, Paul DR. Rheological behavior of multiwalled carbon nanotube/polycarbonate composites. Polymer. 2002;43(11):3247-55.

[56] Kim H, Macosko CW. Processing-property relationships of polycarbonate/graphene composites. Polymer. 2009;50(15):3797-809.

[57] Vermant J, Ceccia S, Dolgovskij MK, Maffettone PL, Macosko CW. Quantifying dispersion of layered nanocomposites via melt rheology. Journal of Rheology. 2007;51(3):429-50.

[58] Treece MA, Oberhauser JP. Soft glassy dynamics in polypropylene-clay nanocomposites. Macromolecules. 2007;40(3):571-82.

[59] Ren J, Casanueva BF, Mitchell CA, Krishnamoorti R. Disorientation kinetics of aligned polymer layered silicate nanocomposites. Macromolecules. 2003;36(11):4188-94.

[60] Mewis J, Spaull AJB. RHEOLOGY OF CONCENTRATED DISPERSIONS. Advances in Colloid and Interface Science. 1976;6(2):173-200.

[61] Sahimi M, Arbabi S. Mechanics of disordered solids. II. Percolation on elastic networks with bond-bending forces. Physical Review B. 1993;47(2):703-12.

[62] Zosel A. Rheological properties of disperse systems at low shear stresses.

Rheologica Acta. 1981;21(1):72-80.

[63] Ren J, Silva AS, Krishnamoorti R. Linear viscoelasticity of disordered polystyrene-polyisoprene block copolymer based layered-silicate nanocomposites. Macromolecules. 2000;33(10):3739-46.

[64] Shante VKS, Kirkpatrick S. An introduction to percolation theory. Adv Phys. 1971;20:325-57.

[65] Benoit JM, Corraze B, Chauvet O. Localization, Coulomb interactions, and electrical heating in single-wall carbon nanotubes/polymer composites. Physical Review B - Condensed Matter and Materials Physics. 2002;65(24):2414051-4.

[66] Garboczi E, Douglas J. Intrinsic conductivity of objects having arbitrary shape and conductivity. Physical Review E. 1996;53(6):6169-80.

[67] Levon K, Margolina A, Patashinsky AZ. Multiple percolation in conducting polymer blends. Macromolecules. 1993;26(15):4061-3.

[68] Surve M, Pryamitsyn V, Ganesan V. Universality in Structure and Elasticity of Polymer-Nanoparticle Gels. Phys Rev Lett. 2006;96.

[69] Arbabi S, Sahimi M. Mechanics of disordered solids. I. Percolation on elastic networks with central forces. Physical Review B. 1993;47(2):695-702.

[70] Filippone G, Salzano De Luna M, Acierno D, Russo P. Elasticity and structure of weak graphite nanoplatelet (GNP) networks in polymer matrices through viscoelastic analyses. Polymer (United Kingdom). 2012;53(13):2699-704.

[71] Chakrabarti K, Nambissan PMG, Mukherjee CD, Bardhan KK, Kim C, Yang KS. Positron annihilation spectroscopy of polyacrylonitrile-based carbon fibers embedded

with multi-wall carbon nanotubes. Carbon. 2006;44(5):948-53.

[72] Kim SH, Chung JW, Kang TJ, Kwak SY, Suzuki T. Determination of the glass transition temperature of polymer/layered silicate nanocomposites from positron annihilation lifetime measurements. Polymer. 2007;48(14):4271-7.

[73] Dammert RM, Maunu SL, Maurer FHJ, Neelov IM, Niemelä S, Sundholm F, et al. Free volume and tacticity in polystyrenes. Macromolecules. 1999;32(6):1930-8.

[74] Sharma SK, Prakash J, Bahadur J, Sudarshan K, Maheshwari P, Mazumder S, et al. Investigation of nanolevel molecular packing and its role in thermo-mechanical properties of PVA-fMWCNT composites: positron annihilation and small angle X-ray scattering studies. Physical Chemistry Chemical Physics. 2014;16(4):1399-408.

[75] Sharma SK, Prakash J, Sudarshan K, Maheshwari P, Sathiyamoorthy D, Pujari PK. Effect of interfacial interaction on free volumes in phenol-formaldehyde resin-carbon nanotube composites: Positron annihilation lifetime and age momentum correlation studies. Physical Chemistry Chemical Physics. 2012;14(31):10972-8.

[76] Patil PN, Sudarshan K, Sharma SK, Maheshwari P, Rath SK, Patri M, et al. Investigation of nanoscopic free volume and interfacial interaction in an epoxy resin/modified clay nanocomposite using positron annihilation spectroscopy. ChemPhysChem. 2012;13(17):3916-22.

[77] Deng Q, Jean YC. Free-volume distributions of an epoxy polymer probed by positron annihilation: Pressure dependence. Macromolecules. 1993;26(1):30-4.